

Numerical Investigation on Effect of Orientation and Rotation on Liquid-Vapor Phase Change around a Cylinder in Staggered Arrangement

Ravi Pullepudi¹, S. K. Maharana²

¹Research Scholar, Research Centre, Department of Mechanical Aeronautical Engineering, MVJ College of Engineering, Bangalore 560067, India.

²Professor, Department of Aeronautical Engineering, Acharya Institute of Technology, Bangalore-560107, India.

Abstract

The complexity of problem of fluid flow and heat transfer over an array of circular cylinders are common in industrial applications of fluid dynamics. The complex nature of the problem encountered in industry gives rise to certain significant dimensions in fluid dynamics theory. Some of them are fluid flow interaction, interferences in flow and vortex dynamics which are typically found in compact heat exchangers, cooling of electronic equipment, nuclear reactor fuel rods, cooling towers, chimney stacks, offshore structures, hot-wire anemometry and flow control.

The mentioned structures are subjected to air or water flows and therefore, experience flow induced forces which can lead to their failure over a long period of time. Basically, with respect to the free stream direction, the configuration of two cylinders can be classified as tandem, side-by-side and staggered arrangements. The Reynolds Averaged Navier-Stokes (RANS) equations are used to compute the flow and Eulerian model is used for to understand phase change situation. The validation of the results was done with that of the literatures. In the present study nucleate boiling has been the cause of heat and mass transfer between the phases. Orientation of cylinders in a specific arrangement has significant impact on phase change and volume fraction of both liquid and vapor phase.

Keywords: RANS, Heat Flux, Phase Change, Eulerian model, Volume Fraction, Staggered Arrangement

1. INTRODUCTION

Many of the outstanding research activities in the domain of fluid flow and heat transfer have expanded by concentrating focus on the effect of spacing between the cylinders on the flow characteristics and heat transfer around them. It was keenly noted that the qualitative nature of the flow depends strongly on the arrangement of cylinders [1-4]. Most of the numerical simulations of flow over a pair of circular cylinders have utilized finite element methods. The problem numerically investigated by Mittal et al. [3] is primarily based on finite element method. The finding of their research was reported for Reynolds numbers of 100 and 1000 for cylinders in staggered and tandem arrangement for various spacings. The conclusion from their study was that the shear layers a $Re=1000$ and $L/D=2.5$ as compared to the case at $Re=100$

caused instability due to the increased velocity of flow. At $Re=100$ the flow was found to be converged to steady state. Increasing the gap to $L/D=5.5$, the flow at $Re=100$ showed unsteady behavior. They indicated that the Strouhal numbers that are associated with the vortex shedding of the twin cylinders could take on the same value.

The available experimental investigations and numerical simulations demonstrated rich hydrodynamic phenomena for the problems of fluid flow over double circular cylinders. In addition to the early experimental investigations, many researchers studied this problem by using numerical simulations. The findings of research done by Li et al. (1991) on two flow patterns for the laminar flow over twin tandem circular cylinders were reported for $Re=100$.

For the large spacing ratio ($L/D>3.0$), the vortices are observed to be shed off from both twin cylinders. For $L/D<3.0$, it was observed that the vortex shedding happens in the downstream of the cylinder and the vortices, slightly out of phase, from the two cylinders rotate in the same direction in their near wake region

The experimental work of Zhang and Melbourn [5], Bearman and Wadcock [6], Liu et al. [7] and Ryu et al. [8] to study wake interaction between two circular cylinders in tandem and side-by-side arrangements were also published subsequently. In their work a flow visualization method was used to study the effect of interference between two circular cylinders in side-by-side arrangement at $Re=2.5 \times 10^4$. By applying unstructured spectral element method to investigate the flow pattern of two side-by-side cylinders for different spacings, Liu et al. [7] carried out their research at low Reynolds numbers.

Mahir and Altac [9], Singha and Sinhamahapatra [10], Ding et al. [11] and Kitagawa and Ohta [12] carried out research using numerical method to investigate flow pattern for tandem arrangement of cylinders for both laminar and turbulent regimes. The three-dimensionality effects were studied numerically in the wake of two fixed tandem cylinders at $Re=220$ by Deng et al. [13]. In their study, virtual boundary method to apply the no-slip condition. From their investigation, like 2 dimensional case, critical spacing range for which instability occurred fell between 3.5 and 4 of L/D . That means for $L/D \leq 3.5$, the flow wake maintained a 2-D state and for $L/D \geq 4$, three-dimensionality effects appeared in the wake.

In fact, among the numerical works done on flow over a pair of cylinders at high Reynolds numbers, one of the most recent significant studies has carried out at $Re = 2.2 \times 10^4$ by Kitagawa and Ohta [12] by simulating a three dimensional flow over two tandem cylinders. The researchers have considered a change of gap of 2D to 4D between the two cylinders, analyzed interference effect and vortex interaction of two cylinders and validated their finding with the experimental data for the same Reynolds number.

Of noticeable experimental works at subcritical Reynolds numbers, one can mention the studies of Ljungkrona et al. [14] at $Re = 2 \times 10^4$ and Moriya et al. [15] at $Re = 6.5 \times 10^4$. They thoroughly investigated the flow characteristics of two tandem cylinders.

The drag forces, pressure distribution, velocity profile, vortex shedding frequency and flow patterns for the twin circular cylinders in a tandem arrangement have been summarized by Zdravkovich [16] in his study.

The intense literature review done above has enormously motivated the authors to understand the phase change phenomenon when water flows over two heated circular cylinders of equal diameters and are in tandem or staggered arrangement kept at different spacing between them and by changing Reynolds number.

2. GOVERNING EQUATIONS

The basic set of governing equations used to solve the multiphase flow problem is given below.

The first step in solving any multiphase problem is to determine which of the regimes provides some broad guidelines for determining appropriate models for each regime, and how to determine the degree of interphase coupling for flows involving bubbles, droplets, or particles, and the appropriate model for different amounts of coupling. Eulerian model is used in the solution of the current problem.

The Eulerian model is the most complex of the multiphase models. It solves a set of momentum and continuity equations for each phase. Coupling is achieved through the pressure and interphase exchange coefficients. The manner in which this coupling is handled depends upon the type of phases involved; granular (fluid-solid) flows are handled differently than non-granular (fluid-fluid) flows.

Volume fraction equation

The description of multiphase flow as interpenetrating continua incorporates the concept of phasic volume fractions, denoted here by α_q . Volume fractions represent the space occupied by each phase, and the laws of conservation of mass and momentum are satisfied by each phase individually.

The volume of phase q is defined by V_q

$$V_q = \int \alpha_q dV \quad (1)$$

Where,

$$\sum_{q=1}^n \alpha_q = 1 \quad (2)$$

The effective density of phase q is $\hat{\rho}_q = \alpha_q \rho_q$

Where ρ_q is the physical density of Phase q . The volume fraction equation may be solved either through implicit or explicit time discretization.

Conservation Equations:

The general conservation equations from which the equations are solved are presented below. The three equations are for conservation of mass, conservation of momentum and energy.

Conservation of mass

The continuity equation for phase q is

$$\frac{\partial}{\partial t} (\alpha_q \rho_q) + \nabla \cdot (\alpha_q \rho_q \vec{v}_q) = \sum_{p=1}^n (\dot{m}_{pq} - \dot{m}_{qp}) + S_q \quad (3)$$

Where \vec{v}_q is the velocity of phase q and \dot{m}_{pq} characterizes the mass transfer from the p^{th} to q^{th} phase, and \dot{m}_{qp} characterizes the mass transfer from phase q to phase p . By default, the source term S_q on the right-hand side of the above equation is zero, but we can specify a constant or user-defined mass source for each phase.

Conservation of Momentum

The momentum balance for phase q yields

$$\begin{aligned} \frac{\partial}{\partial t} (\alpha_q \rho_q \vec{v}_q) + \nabla \cdot (\alpha_q \rho_q \vec{v}_q \vec{v}_q) \\ = -\alpha_q \nabla p + \nabla \cdot \bar{\tau}_q + \alpha_q \rho_q \vec{g} + \\ \sum_{p=1}^n (\vec{R}_{pq} + \dot{m}_{pq} \vec{v}_{pq} - \dot{m}_{qp} \vec{v}_{qp}) + (\vec{F}_q + \vec{F}_{lift,q} + \vec{F}_{vm,q}) \end{aligned} \quad (4)$$

Where

$$\bar{\tau}_q = \alpha_q \mu_q (\nabla \vec{v}_q + \nabla \vec{v}_q^T) + \alpha_q \left(\lambda_q - \frac{2}{3} \mu_q \right) \nabla \cdot \vec{v}_q \bar{I} \quad (5)$$

This is q^{th} phase stress-strain tensor.

Here μ_q and λ_q are the shear and bulk viscosity of phase q , \vec{F}_q is an external body force, $\vec{F}_{lift,q}$ is a lift force, $\vec{F}_{vm,q}$ is a virtual mass force, \vec{R}_{pq} is an interaction force between phases, and p is the pressure shared by all phases.

\vec{v}_{pq} is the interphase velocity, defined as follows: If \dot{m}_{pq} (i.e., phase p mass is being transferred to phase q), $\vec{v}_{pq} = \vec{v}_p$;

if $\dot{m}_{pq} < 0$ (i.e., phase q mass is being transferred to phase p), $\vec{v}_{pq} = \vec{v}_q$. Likewise, if $\dot{m}_{qp} > 0$ then $\vec{v}_{qp} = \vec{v}_q$, if $\dot{m}_{qp} < 0$ then $\vec{v}_{qp} = \vec{v}_p$.

Equation 4 must be closed with appropriate expressions for the interphase force, \vec{R}_{pq} . This force depends on the friction, pressure, cohesion, and other effects, and is subject to the conditions that $\vec{R}_{pq} = -\vec{R}_{qp}$ and $\vec{R}_{qq} = 0$

The interaction term of the following form:

$$\sum_{p=1}^n \vec{R}_{pq} = \sum_{p=1}^n K_{pq} (\vec{v}_p - \vec{v}_q)$$

Where K_{pq} ($= K_{qp}$) is the interphase momentum exchange coefficient.

Conservation of Energy

Conservation of energy in Eulerian multiphase applications. The current problem uses this form of the equation

$$\begin{aligned} \frac{\partial}{\partial t} (\alpha_q \rho_q h_q) + \nabla \cdot (\alpha_q \rho_q \vec{u}_q h_q) \\ = -\alpha_q \frac{\partial p_q}{\partial t} + \bar{\tau}_q : \vec{u}_q - \nabla \cdot \vec{q}_q \\ + S_q + \sum_{p=1}^n (Q_{pq} + \dot{m}_{pq} h_{pq} \\ - \dot{m}_{qp} h_{qp}) \end{aligned} \quad (7)$$

where is h_q the specific enthalpy of the q^{th} phase, \vec{q}_q is the heat flux, S_q is a source term that includes sources of enthalpy (e.g., due to chemical reaction or radiation), Q_{pq} is the intensity of heat exchange between the p^{th} and q^{th} phases, and h_{pq} is the interphase enthalpy (e.g., the enthalpy of the vapor at the temperature of the droplets, in the case of evaporation). The heat exchange between phases must comply with the local balance conditions $Q_{pq} = -Q_{qp}$ and $Q_{pq} = 0$.

Turbulence Models

In comparison to single-phase flows, the number of terms to be modeled in the momentum equations in multiphase flows is large, and this makes the modeling of turbulence in multiphase simulations extremely complex. One of the three methods for modeling turbulence in multiphase flows within the context of $k - \epsilon$ models are mixture turbulence models. The description of mixture turbulence model is presented below.

$k - \epsilon$ Mixture Turbulence Model

The mixture turbulence model is the default multiphase turbulence model. It represents the first extension of the

single-phase $k - \epsilon$ model, and it is applicable when phases separate, for stratified (or nearly stratified) multiphase flows, and when the density ratio between phases is close to 1. In these cases, using mixture properties and mixture velocities is sufficient to capture important features of the turbulent flow.

The k and ϵ equations describing this model are as follows:

$$\frac{\partial}{\partial t} (\rho_m k) + \nabla \cdot (\rho_m \vec{v}_m k) = \nabla \cdot \left(\frac{\mu_{t,m}}{\sigma_k} \nabla k \right) + G_{k,m} - \rho_m \epsilon \quad (8)$$

and

$$\frac{\partial}{\partial t} (\rho_m \epsilon) + \nabla \cdot (\rho_m \vec{v}_m \epsilon) = \nabla \cdot \left(\frac{\mu_{t,m}}{\sigma_\epsilon} \nabla \epsilon \right) + \frac{\epsilon}{k} (C_{1\epsilon} G_{k,m} - C_{2\epsilon} \rho_m \epsilon) \quad (9)$$

Where the mixture density ρ_m and velocity \vec{v}_m are computed from

$$\rho_m = \sum_{i=1}^N \alpha_i \rho_i \quad (10)$$

and

$$\vec{v}_m = \frac{\sum_{i=1}^N \alpha_i \rho_i \vec{v}_i}{\sum_{i=1}^N \alpha_i \rho_i} \quad (11)$$

The turbulent viscosity, $\mu_{t,m}$ is computed from

$$\mu_{t,m} = \rho_m C_\mu \frac{k^2}{\epsilon} \quad (12)$$

and the production of turbulence kinetic energy, $G_{k,m}$ is computed from

$$G_{k,m} = \mu_{t,m} (\nabla \vec{v}_m + (\nabla \vec{v}_m)^T) : \nabla \vec{v}_m \quad (13)$$

The constants in these equations are given below for the single-phase $k - \epsilon$ model.

$$C_\mu = 0.09, C_{1\epsilon} = 1.44, C_{2\epsilon} = 1.92, \sigma_k = 1.0, \sigma_\epsilon = 1.3$$

3. METHODOLOGY

A sketch definition of numerical set-up (shown in x-y plane) for two circular cylinders in tandem arrangement with boundary conditions is shown in the Fig.1. The necessary dimensions of the fluid domain are expressed in terms of the diameter (D) of a cylinder. The diameters of both the cylinders are the same. The two cylinders are arranged in tandem inside the flow domain. The mesh density is higher near the walls of cylinders. The total number of nodes of the mesh generated is 5117 and that of elements is 3984. The flow enters at **inlet** where the inlet velocity is specified ($u=U$) and leaves the domain at **outlet**. The temperature at the cylinder surface is maintained at 573 K. All walls are stationary and have no slip boundary conditions.

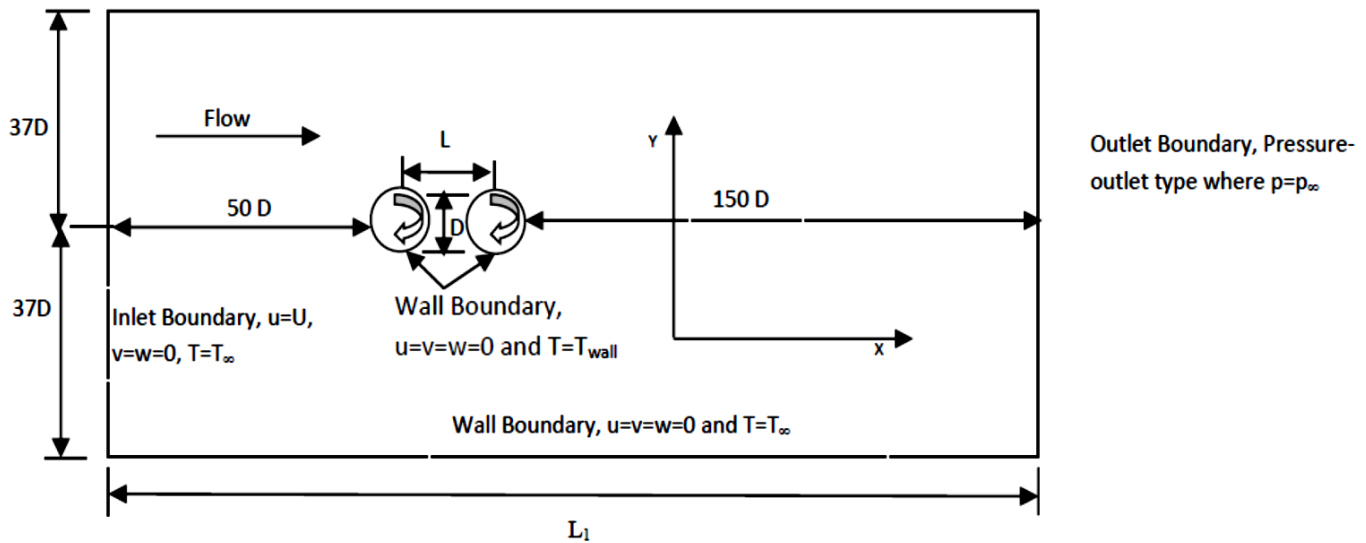


Fig.1: Physical Domain (shown in x-y plane) for two circular cylinders with boundary conditions

The commercial computational fluid dynamics (CFD) solver Ansys^(R)Fluent was used for the simulation of fluid flow and heat transfer over the cylinders. The working fluid is water (liquid phase), upon phase change, becomes steam (vapor phase).

4. RESULTS AND DISCUSSIONS

The effect of orientation of a cylinder in an arrangement and its rotation on the volume fraction of each phase has been the focus. Hence two different arrangements such as tandem and staggered are considered during the computation to understand the phase change of liquid to vapor phase over a cylinder whose surface is heated to a certain temperature (above the saturation temperature of vapor).

Rotation of cylinders was considered during the simulation to assess how it affects the volume fraction of both the phases. The rate of rotation of a cylinder (indicated by α) is denoted by $D\omega/2U_\infty$, where U_∞ is the free-stream velocity and D is the diameter of cylinder and ω is its angular velocity.

There has been a validation of a few quantities such as the mean drag coefficient, mean lift coefficient and Strouhal numbers of the isolated circular cylinder with that of the other researchers and the details are mentioned in the **Table 1**. In the **Fig.2** is plotted the mean drag coefficient versus Re of the flow.

The comparison of the present values of mean drag coefficient with the data published earlier is fairly good. The comparison of the non-dimensional quantities such as Mean drag coefficient, C_D^M , mean lift coefficient C_L^M and Strouhal number, St was done with those published by leading researchers and

the authors, due to good comparison and validation of the above-mentioned quantities, have carried out their study to investigate the flow over two heated circular cylinders

Table 1: Comparison of the mean drag coefficient C_D^M , C_L^M and St

	C_D^M	C_L^A	St
Present	1.41	0.692	0.1902
M-M Lui <i>et al.</i> (2014)	1.337	0.685	0.1955
B.N. Rajani <i>et al.</i> (2009)	1.3380	0.4276	0.1936
Wang <i>et al.</i> (2009)	-	0.71	0.1950
Zhang <i>et al.</i> (2008)	1.34	0.66	0.1970
Linnick and Fascl (2005)	1.34-1.37	0.71	-
Farrani <i>et al.</i> (2001)	1.36-1.39	0.71	-
He <i>et al.</i> (2000)	1.36	-	0.1978
Data compiled by Zdravkovich (1997)	1.43	-	-
Henderson (1995)	1.34-1.37	-	0.1971

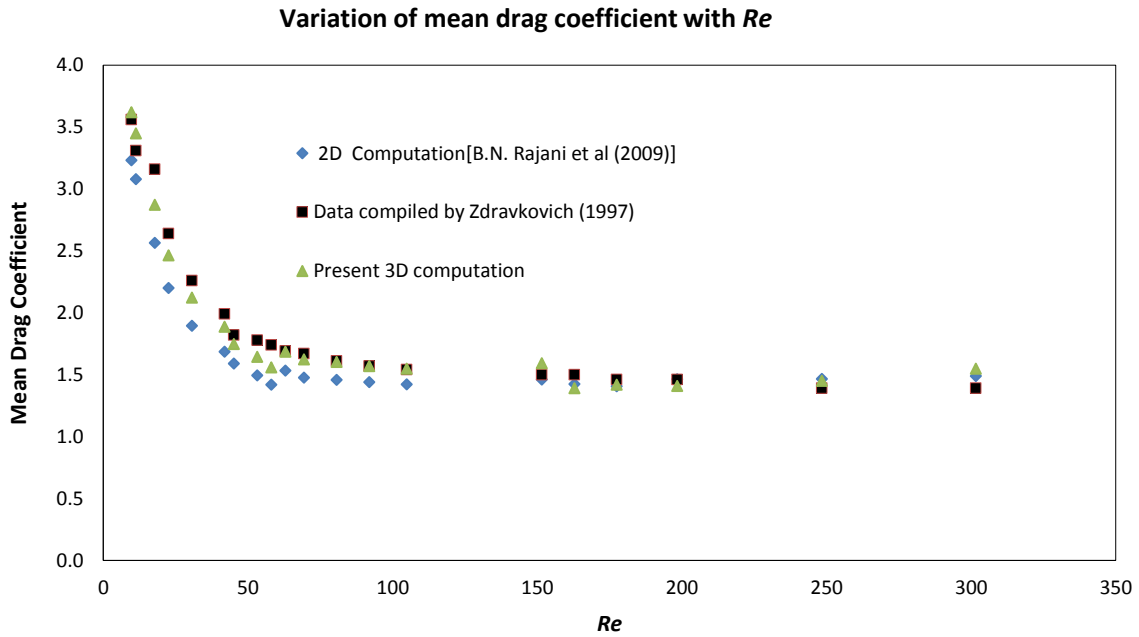


Fig.2: Comparison of Mean Drag Coefficients for various Reynolds number for a single circular cylinder

Phase Change of Liquid to Vapor:

In Fig.3 (a) is shown the contours of liquid-vapor phase for two non-rotating cylinders in tandem arrangement and Fig.3 (b) shows the variation of volume fraction (VOF) of vapor around the same two cylinders shown in Fig.3(a). The range of variation of VOF is between 0.5 and 0.9 around both the cylinders and it is noted that cylinder-1 [extreme left one] experiences more vapor at a location of 120° on its surface and cylinder-2 faces more vapor at a location around 350° on its surface.

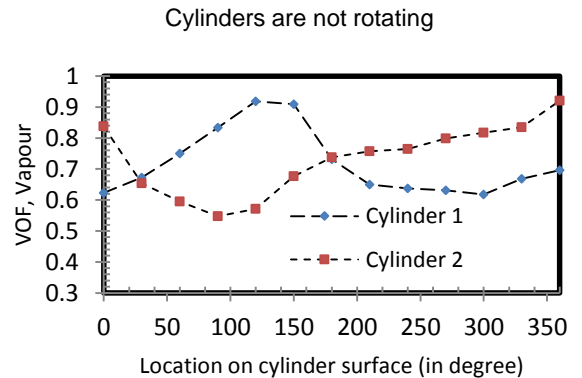


Fig.3(b) Variation of VOF of vapor around two cylinders shown in Fig.4(a)

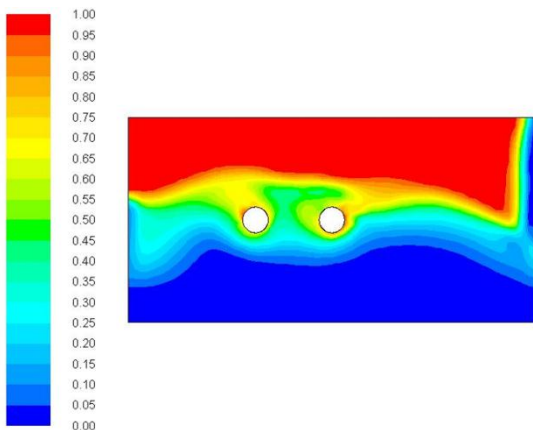


Fig.3(a) Contours of liquid-vapor phase for two non-rotating cylinders in tandem

In Fig.4(a) is shown the contours of liquid-vapor phase for two rotating cylinders in tandem arrangement and Fig.4(b) shows the variation of volume fraction (VOF) of vapor around the same two cylinders shown in Fig.4(a). The range of variation of VOF varies between 0.51 and 0.95 around cylinder-1 and the variation of VOF is between 0.67 and 0.89 for cylinder-2. It is noted that cylinder-1 [extreme left one] experiences more vapor at a location of 50° on its surface and cylinder-2 faces more vapor at a location around 350° on its surface.

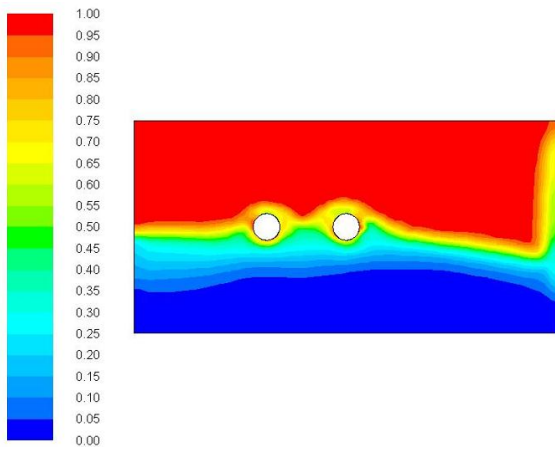


Fig.4(a) Contours of liquid-vapor phase for two rotating cylinders in tandem

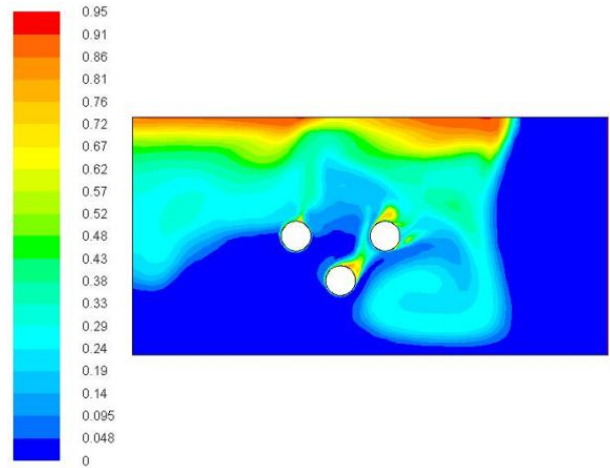


Fig.5(a) Contours of liquid-vapor phase for three non-rotating cylinders in staggered arrangement

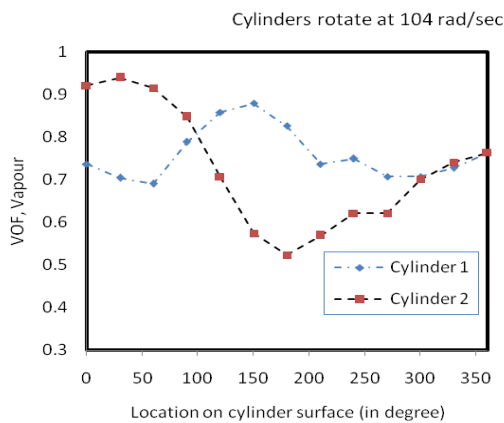


Fig.4(b) Variation of VOF of vapor around two cylinders shown in Fig.5(a)

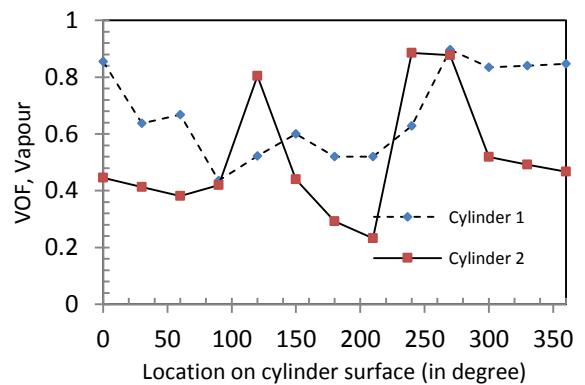


Fig.5(b) Variation of VOF of vapor around two cylinders [extreme left and extreme right] shown in Fig.5(a)

In Fig.5(a) is shown the contours of liquid-vapor phase for three non-rotating cylinders in staggered arrangement and Fig.5(b) shows the variation of volume fraction (VOF) of vapor around the two cylinders [extreme left and right] shown in Fig.5(a). By introducing another cylinder in the arrangement described in Fig.4(a) a new staggered arrangement was made which is shown in Fig.5(a). The arrangement has significantly affected the phase interaction between the liquid and vapor phases. There is a lowering of VOF (~0.2) in cylinder-2 and the VOF for cylinder-1 has also been affected (increased) by 10-15%. It is also observed that more time is needed for a better VOF to be seen around the cylinders at hand.

The range of variation of VOF varies between 0.4 and 0.9 around cylinder-1 and the variation of VOF is between 0.2 and 0.85 for cylinder-2. It is noted that cylinder-1 [extreme left one] experiences more vapor at a location of 0° and 350° on its surface and cylinder-2 faces more vapor at a location around 200° on its surface.

In Fig.6(a) is shown the contours of liquid-vapor phase for four non-rotating cylinders in staggered arrangement and Fig.6(b) shows the variation of volume fraction (VOF) of vapor around the two cylinders [extreme left and right] shown in Fig.6(a). By introducing another cylinder in the arrangement described in Fig.6(a) a new staggered arrangement was made which is shown in Fig.6(a). The arrangement has significantly affected the phase interaction between the liquid and vapor phases. There is an enhancement of VOF (~0.4 in the lower side and ~1.0 in the upper side) in cylinder-2 and the VOF for cylinder-1 has also been affected by 5%. The range of variation of VOF varies between 0.45 and 0.9 around cylinder-1 and the variation of VOF is between 0.41 and 1.0 for cylinder-2. It is noted that cylinder-2 [extreme right one] experiences more vapor at a location of 0° on its surface and cylinder-1 faces more vapor at a location around 130° on its surface.

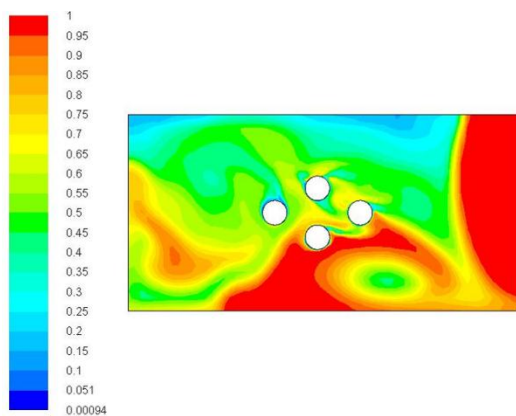


Fig.6(a) Contours of liquid-vapor phase for four non-rotating cylinders in staggered arrangement

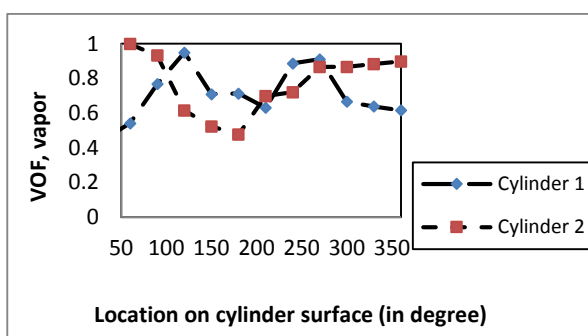


Fig.6(b) Variation of VOF of vapor around two cylinders[extreme left and extreme right]shown in Fig.6(a)

5. CONCLUSION

The effect of orientation of a cylinder on liquid-vapor phase change has been studied. The rotation of a cylinder on the VOF has also been noted during the study. A comparison of VOF of vapor over a cylinder was made for two separate arrangements of cylinders. In the staggered arrangement the rise of VOF by 15% for both the cylinders was noteworthy. The rotation has enhanced the VOF by around 20% around both the cylinders. The heat and mass transfer during liquid-vapor phase change have been enhanced with the nucleate boiling phenomenon which was the mechanism of phase interaction.

REFERENCES

- [1] Zdravkovich M.M., Flow around circular cylinders, fundamentals, vol. 1, Oxford University Press, London, 1997.
- [2] Zdravkovich M.M., Flow around circular cylinders, fundamentals, vol. 1, Oxford University Press, London, 2003.
- [3] Mittal S., Kumar V., Raghuvanshi A., Unsteady incompressible flows past two cylinders in tandem and staggered arrangements, Int. J. Numer. Methods Fluid 25 (1997) 1315–1344.
- [4] Meneghini J.R., Saltara F., Siqueira C.L.R., Ferrari Jr J.A., Numerical simulation of flow interference between two circular cylinders in tandem and side-by-side arrangements, J. Fluids Struct. 15 (2001) 327–350.
- [5] Zhang H., Melbourne W. H. Interference between two circular cylinders in tandem in turbulent flow. Journal of Wind Engineering and Industrial Hydrodynamics, 1992, 41(1-3): 589-600.
- [6] Bearmann P. W., Wadcock A. J. The interaction between a pair of circular cylinders normal to a stream. J. Fluid Mech., 1973, 61: 499-511.
- [7] Liu Kun, Ma Dong-jun and Sun De-jun et al., Wake patterns of flow past a pair of circular cylinders in side by-side arrangements at low Reynolds numbers. J. Hydrodynamics, Ser. B, 2007, 19(6): 690-697.
- [8] Ryu S., Lee S. B. and Lee B. H. et al., Estimation of hydrodynamic coefficients for flow around cylinders in side-by-side arrangement with variation in separation gap, Journal of Ocean Engineering, 2009, 36(9-10): 672-680.
- [9] Mahir N., Altac Z., Numerical investigation of convective heat transfer in unsteady flow past two cylinders in tandem arrangements, International Journal of Heat and Fluid Flow, 2008, 29(5):1309-1318.
- [10] Singha S., Sinhamahapatra K. P., High resolution numerical simulation of low Reynolds number incompressible flow about two cylinders in tandem. Journal of Fluids Engineering, ASME, 2010, 132(1): 011101.
- [11] Ding H., Shu C. and Yeo K. S. et al., Numerical simulation of flows around two circular cylinders by mesh-free least square-based finite difference methods. International Journal for Numerical Methods in Fluids, 2007, 53(2): 305-332.
- [12] Kitagawa T., Ohta H., Numerical investigation on flow around circular cylinders in tandem arrangement at a subcritical Reynolds number. Journal of Fluids and Structures, 2008, 24(5): 680-699.
- [13] Deng Jian, Ren An-lu and Chen Wen-qu., Numerical simulation of flow-induced vibration on two circular cylinders in tandem arrangement, Journal of Hydrodynamics, Ser. B, 2005, 17(6): 660-666.
- [14] Ljungkrona L., Norberg C. and Sundén B., Free-stream turbulence and tube spacing effects on surface pressure fluctuations for two tubes in an in-line arrangement, Journal of Fluids and Structures, 1991, 5(6): 701-727.
- [15] Moriya M., Alam M. and Takai K. et al., Fluctuating fluid forces of two circular cylinders in tandem arrangement at close spacing, Transactions of the Japan Society of Mechanical Engineers, 2002, 68(669): 1400-1406.

- [16] Zdravkovich M M, Review of flow interference between two circular cylinders in various arrangements, *J. Fluids Eng.*, 1977, 37 993-1010
- [17] Ming-Ming Liu et al., Re-examination of laminar flow over twin circular cylinders in tandem arrangement, 2014, *Fluid Dynamics Research* 48 1-21
- [18] Rajani B.N., Kandaswamy A and SekharManjumdar, Numerical simulation of laminar flow past a circular cylinder, 2009, *Applied Mathematical Modelling*, 33 1228-1247
- [19] Wang ZL, Fun J R and Cen K F , Immersed boundary method for the simulation of 2D viscous flow based on vorticity-velocity formulations , 2009, *J. Comput. Phys.* 228 1504-1520
- [20] Zhang X, Ni S Z and He G W, A pressure correction method and its applications on an unstructured Chimera grid , 2008 *Comput. Fluids.* 37 993-1010.
- [21] Linnick M N and Fasel H F, A high-order immersed interface method for simulating unsteady incompressible flows on irregular domains, 2005, *J. Comput. Phys.* 204 157-192
- [22] He J W, Glowinski R, Motcalfe R, Nordlander A and Periaux J, Active control and drag optimization for flow past a circular cylinder, 2000, *J. Comput. Phys.*, 163 83-117.
- [23] Farrani T, Tan M and Price W G, A cell boundary element method applied to laminar vortex shedding from circular cylinder, 2001, *Comput. Fluids* 30 211-236
- [24] Henderson R D, Details of the drag curve near the onset of vortex shedding, 1995, *Phys. Fluids* 7 2102-2104